JOURNAL OF GEOPHYSICAL RESEARCH, VOL. 88, NO. B3, PAGES 2431-2444, MARCH 10, 1983

SHOCK TEMPERATURES OF SiO_2 AND THEIR GEOPHYSICAL IMPLICATIONS

Gregory A. Lyzenga[1] and Thomas J. Ahrens

Seismological Laboratory, California Institute of Technology, Pasadena, California 91125

Arthur C. Mitchell

Lawrence Livermore National Laboratory, Livermore, California 94550

Abstract. The temperature of SiO_2 in high-pressure shock states has been measured for samples of single-crystal α-quartz and fused quartz. Pressures between 60 and 140 GPa have been studied using projectile impact and optical pyrometry techniques at Lawrence Livermore National Laboratory. Both data sets indicate the occurrence of a shock-induced phase transformation at ~70 and ~50 GPa along the α- and fused quartz Hugoniots, respectively. The suggested identification of this transformation is the melting of shock-synthesized stishovite, with the onset of melting delayed by metastable superheating of the crystalline phase. Some evidence for this transition in conventional shock wave equation of state data is given, and when these data are combined with the shock temperature data, it is possible to construct the stishovite-liquid phase boundaries. The melting temperature of stishovite near 70 GPa pressure is found to be 4500 K, and melting in this vicinity is accompanied by a relative volume change and latent heat of fusion of ~2.7% and ~2.4 MJ/kg, respectively. The solid stishovite Hugoniot centered on α-quartz is well described by the linear shock velocity-particle velocity relation, $u_s = 1.822\ u_p + 1.370$ km/s, while at pressures above the melting transition, the Hugoniot centered on α-quartz has been fit with $u_s = 1.619\ u_p + 2.049$ km/s up to a pressure of ~200 GPa. The melting temperature of stishovite near 100 GPa suggests an approximate limit of 3500 K for the melting temperature of SiO_2-bearing solid mantle mineral assemblages, all of which are believed to contain Si^{4+} in octahedral coordination with O^{2-}. Thus 3500 K is proposed as an approximate upper limit to the melting point and the actual temperature in the earth's mantle. Moreover, the increase of the melting point of stishovite with pressure at 70 GPa is inferred to be ~11 K/GPa. Using various adiabatic temperature gradients in the earth's mantle and assuming creep is diffusion controlled in the lower mantle, the current results could preclude an increase of viscosity by more than a factor of 10^3 with depth across the mantle.

Introduction

The properties of silica and its high-pressure polymorphs have long been of interest because of their bearing on problems of the physical and compositional states of the earth's interior. Models of the high-pressure equation of state and phase diagram of SiO_2 may provide direct information about candidate mantle mineral assemblages, because SiO_2 readily transforms to a rutilelike phase (stishovite) above 14 GPa, in which Si^{4+} has octahedral oxygen coordination. It would therefore appear to be a useful guide for the study of other lower mantle octahedrally coordinated silicates. Modern techniques for the dynamic compression of minerals [Ahrens, 1980] are providing such data at pressures near 100 GPa, which are appropriate to the state of the earth's lower mantle and core.

Shock wave compression of solids depends upon the generation and propagation of a planar, steady pressure step in the material of interest. As described elsewhere [e.g., Davison and Graham, 1979], the time independent profile of this pressure discontinuity or shock front in one-dimensional flow allows application of the Rankine-Hugoniot (R-H) conservation equations, which relate pressure P, density ρ, and energy E, of the compressed state to the shock and mass velocities of the flow. The Hugoniot curve, or locus of (P, ρ, E) states accessible to a given material when shocked, is thus measurable through observations of shock wave propagation. One technique for producing and characterizing such shocks is the method of flying plate impact, through the use of a two-stage gas gun [Jones et al., 1966]. This apparatus accelerates projectiles bearing metallic flyer plates to speeds of up to 7 km/s, which upon impact induce shock pressures in silicate specimens in excess of 150 GPa.

Hugoniot temperature measurements can provide an important source of data specifying the thermal pressure component of the equation of state, which is not explicitly obtainable from the R-H conservation equations. The present optical pyrometry method for shock temperature measurement, developed jointly with Lawrence Livermore Laboratory, is applicable to transparent materials and has been used to demonstrate how the thermal behavior and energy associated with the phase changes in forsterite and silica may be constrained [Lyzenga and Ahrens, 1979, 1980]. The new data and analysis of measured shock temperatures in SiO_2, when taken with the independent work of R. G. McQueen et al. (unpublished data, 1980), provide important new information about the high-pressure phases of SiO_2, which may be applied directly in placing an absolute upper limit on the temperature in the earth's mantle and indirectly in providing the basis for estimation of the melting point of the lower mantle, and thus its creep viscosity.

[1]Now at Jet Propulsion Laboratory, Pasadena, California 91109.

Paper number 2B1880.
0148-0227/83/002B-1880$05.00

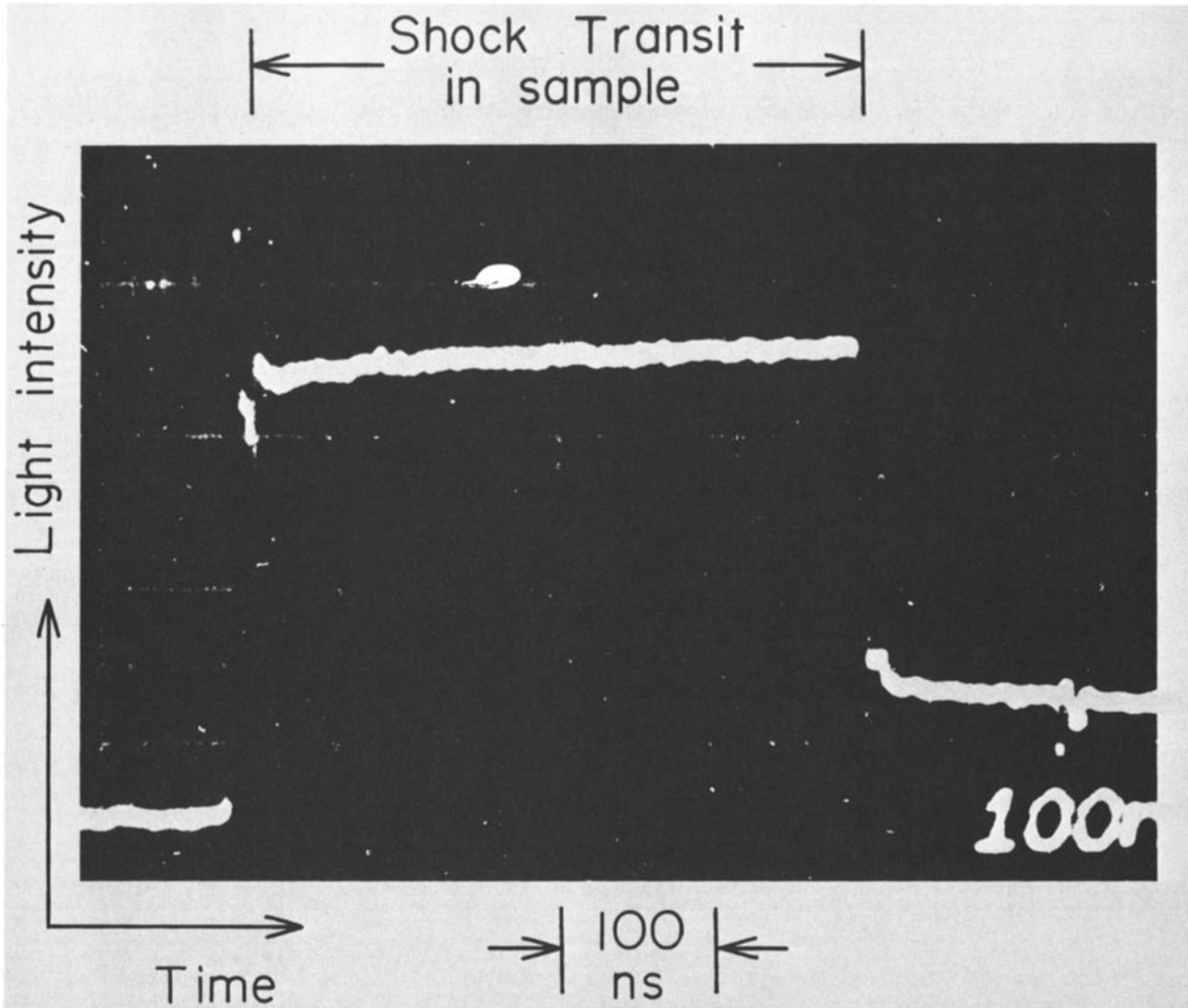

Fig. 1. Oscilloscope record of shock-induced light intensity versus time. Record is taken through 650-nm wavelength interference filter from a fused quartz shot at 68.5 GPa pressure. Each shot results in six such records at wavelengths of 450, 500, 550, 600, 650, and 800 nm. The spectral radiance calibration for this channel is approximately 3.9×10^3 W m^{-2} sr^{-1} nm^{-1} per division.

Experimental Procedures

Samples of single-crystal and fused quartz were driven to shock pressures in the range from 60 to 140 GPa via impact of 2-mm-thick flyer plates accelerated to speeds of from 4.5 to 6.7 km/s using the two-stage light gas gun facility at Lawrence Livermore Laboratory. Thermal radiation emitted by the shocked samples during the period (approximately 300 to 400 ns) of shock wave transit were measured by the pyrometer at each of six visible wavelengths simultaneously [Lyzenga and Ahrens, 1979].

Figure 1 shows the reproduced oscilloscope record from a typical fused quartz experiment and illustrates the manner in which the spectral radiance and duration of shock transit in the sample are derived from the records. Discussed elsewhere [Lyzenga, 1982] is the relation between the observed thermal radiation in this experimental configuration and the equilibrium temperature of the shock compressed state. It suffices here to state that the experimental data are treated under the assumption that the radiated spectrum is a thermal distribution, with an effective emissivity less than or equal to unity. Shock velocities derived from these data have a relative uncertainty of approximately ±1%, which is determined by the amount of shock front tilt and by the limited time resolution of the electronics.

The results of nine shots on single-crystal α-quartz are summarized in Table 1. The samples used in this series of experiments were synthetic quartz crystals with an initial density of 2.648 g/cm^3, supplied by the Adolf Meller Co. The prepared samples were discs approximately 3 mm in thickness by 17 mm in diameter, polished to optical smoothness. Shots were carried out on crystals oriented with the (0001) axis both parallel and perpendicular to the direction of shock propagation, as noted in Table 1. The α-quartz experiments were carried out at pressures between approximately 75 and 140 GPa, in a range

where stishovite has been previously assumed to be the stable solid phase of SiO_2 [McQueen et al., 1963]. As is discussed below, the shock temperature data show that a temperature decline in excess of 1000 K occurs between pressures of 107 and 117 GPa. This temperature drop is illustrated graphically in Figure 2 and is taken as evidence of a shock-induced phase transition of stishovite to another phase.

Table 2 summarizes the results of seven shots carried out with samples of fused silica. The polished discs had an initial density of 2.204 g/cm^3 and were supplied by Amersil Corp. The pressure range studied was 58 to 108 GPa. As in the case of α-quartz, the fused quartz temperature data show evidence for a phase change of the shock-induced stishovite to another phase. Evidence of a similar temperature drop is observed, although at a lower pressure than in the α-quartz experiments.

As seen in the plot of Figure 3, the behavior in the region of temperature decline of fused quartz near 65-70 GPa pressure appears similar to that of α-quartz. The two anomalous temperature segments, however, do not connect to form a continuous curve, as would be expected if they delineate an equilibrium phase boundary. In such a case, the Hugoniot would coincide with the phase line through the region of mixed phases, moving into the high-pressure phase region at higher shock pressures [Duvall and Graham, 1977]. In any case, it is assumed here that all differences between the Hugoniot curves for α-quartz and fused silica result from the different initial densities and consequently different internal energies of SiO_2 shocked from the two different starting phases. Also plotted in Figures 2 and 3 are the calculated Hugoniot temperature curves for α-quartz and fused quartz, assuming that both Hugoniot curves are for SiO_2 in the crystalline stishovite phase. The details of this calculation

TABLE 1. Alpha-quartz Hugoniot Temperatures

Shock Pressure, GPa	Temperature, K
75.9 ± 0.8[a]	4435 ± 40
85.9 ± 1.0[b]	4840 ± 135
92.5 ± 1.0[a]	5395 ± 125
99.3 ± 1.0[a]	5590 ± 170
107.8 ± 1.0[b]	5840 ± 235
109.7 ± 1.0[a]	6030[c]
116.5 ± 1.0[b]	4900 ± 110
126.6 ± 1.0[a]	5295 ± 105
137.0 ± 1.0[b]	5720 ± 130

[a]Shock propagation perpendicular to (0001) axis.

[b]Shock propagation parallel to (0001) axis.

[c]Temperature based upon only two wavelength radiance measurements instead of six.

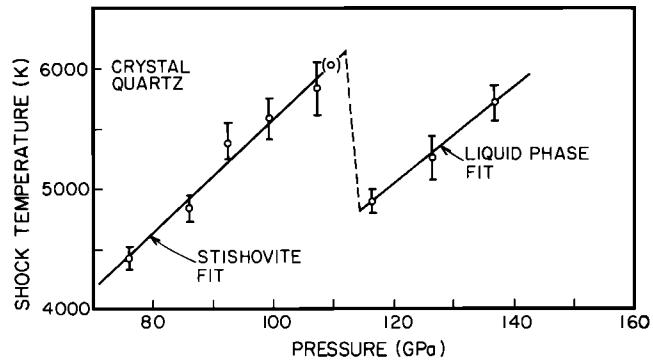

Fig. 2. Measured shock temperatures versus pressure from experiments on single-crystal α-quartz. Open circles represent pyrometer measurements, while heavy lines represent calculated temperatures assuming solid and liquid phases. These calculations employ a temperature dependent specific heat, in order to fit the observations.

are discussed below. The calculated curves are sensitive to the assumed values of E_{tr}, the heat of transition at standard conditions for stishovite from the initial phases. The values assumed here are 0.822 MJ/kg and 0.697 MJ/kg for α-quartz and fused silica, respectively, as measured calorimetrically [Robie et al., 1978]. The Grüneisen parameter $\gamma(V)$ was assumed to be given by the form $\gamma_o(V/V_o)^n$, where $\gamma_o = 1.38$ and $n = 3.2$; γ_o is derived directly from thermodynamic measurements [Ito et al., 1974], and the volume variation given by n comes from requiring γ to describe the shock wave data for both fused and crystalline quartz. It is notable that in both materials the measured Hugoniot temperature curves show reasonable agreement with calculations which assume stishovite is present at pressures below the observed transitions, and that above these transitions the Hugoniot temperatures lie well below the temperatures which are calculated for the solid phase. These observations lend support to the view that the peculiar temperature behavior seen in both materials signals the same phase transition from stishovite to a new phase, even though the transition is apparently not accomplished under equilibrium conditions.

As is discussed by R. G. McQueen et al. (unpublished data, 1980), a shock wave which decreases in amplitude with time may be used to investigate the anomalous region of decreasing temperature. Those investigators observed the radiation from a decaying shock front in fused quartz and noted that the expected temperature reversal does indeed occur. We have confirmed this interesting phenomenon in a single experiment we performed in which a thin flying impactor plate was employed to generate a decaying shock front [Fowles, 1960] in the fused quartz sample. As seen in Figure 4a, the radiation intensity from the sample initially falls and then rises before extinguishing as the shock pressure falls in amplitude. The thermodynamic path traced out by the radiating shock front is along the Hugoniot, rather than along a release adiabat, since at a given instant the material being viewed by the pyrometer is newly shocked material which is immediately behind the front and has just achieved

TABLE 2. Fused Quartz Hugoniot Temperatures

Shock Pressure, GPa	Temperature, K
58.9 ± 1.0	4950 ± 100
68.5 ± 1.0	5095 ± 105
73.3 ± 1.0	4600 ± 75
81.2 ± 1.0	5070 ± 70
93.2 ± 1.5	5730 ± 165
104.2 ± 2.0	6460 ± 220
109.9 ± 2.0	6990 ± 355

the amplitude of the decaying wave at that instant. In the illustrated experiment, the initial shock pressure is 97.5 GPa, and as the pressure falls, the material passes continuously through states on the Hugoniot including the phase transition.

According to the data in Figure 3, the temperature reversal is expected at a pressure of ~70 GPa. Figure 4b shows the intensity record from another fused quartz shot, in this case with constant shock amplitude. At the pressure of this shot, 73 GPa, the material is evidently at or near the temperature minimum which signals the switch from the anomalous transition region to the higher-pressure phase. Unusual quasi-periodic small jumps in intensity are observed during the shock wave transit. This behavior was not observed in identical experimental configurations at different pressures and could not be otherwise reproduced with the electronics and cabling of the experiment, thus apparently ruling it out as an instrumental effect other than random noise. This behavior is analogous to the oscillating optical signal reported by R. G. McQueen et al. (unpublished data, 1980) in the same pressure range and may be related to the metastability of stishovite near the phase transition pressure.

This possibility of a shock-induced phase transition suggests that other evidence for such a transition in the Hugoniot data should be sought. Alpha-quartz is the best candidate for such a search, since the higher initial density reduces the shock heating and hence the masking effect of thermal pressure relative to the case of fused silica. The previously published Hugoniot data for α-quartz have been obtained at pressures below approximately 100 GPa [Wackerle, 1962; R. G. McQueen et al., unpublished data, 1980], and several high-pressure points were obtained above ~200 GPa [Trunin et al., 1971]. These discrete data do not fall within the region of the inferred phase change, so in the present study we have used shock transit times from temperature experiments in addition to conventional streak camera experiments to obtain additional points between 90 and 140 GPa. These data are listed in Table 3, and a summary of all α-quartz data above the stishovite transition (~40 GPa) is presented in a plot of shock velocity versus particle velocity in Figure 5. The improved Hugoniot data obtained for both α-quartz and fused silica have resulted in small corrections to the pressures in the shock temperature experiments, thus accounting for differences between the pressures reported here and those of Lyzenga and Ahrens [1980].

The data for experiments below the 117-GPa completion pressure of the transition seen in the temperature plots are well fitted by a linear u_s-u_p relation of the form

$$u_s = S\, u_p + C_o \qquad (1)$$

As given in the summary of Table 4, in this range the best fit is given by S = 1.822 and C_o = 1.370 km/s. This agrees with the fit assigned by R. G. McQueen et al. (unpublished data, 1980), of S = 1.850 ± 0.045 and C_o = 1.241 ± 0.160 km/s. In contrast, the Hugoniot points from experiments at pressures higher than the new transition do not fall on this extrapolated linear fit. While the limited data available do not absolutely exclude the possibility of fitting the Hugoniot data with a single smooth curve, we have fit the higher-pressure points with another linear segment of shallower slope. The fit line shown in Figure 5 is given by S = 1.619 and C_o = 2.049 km/s, also listed in Table 4.

Besides the shallower slope on the high-pressure branch, this two-segment fit yields a discontinuity between the two branches, rather than a smooth joining of the two where the break in slope occurs. The proposed discontinuity in the shock velocity-particle velocity function implies an approximately 2% discontinuous increase in density. It is of interest to note that if extrapolated back into the low-pressure region, the high-pressure fit would intersect the steeper low-pressure fit in the neighborhood of u_p = 3.5 km/s, corresponding to a shock pressure of about 70 GPa. As discussed below, this turns out to be the pressure of the onset of the equilibrium phase transition, as inferred on independent grounds.

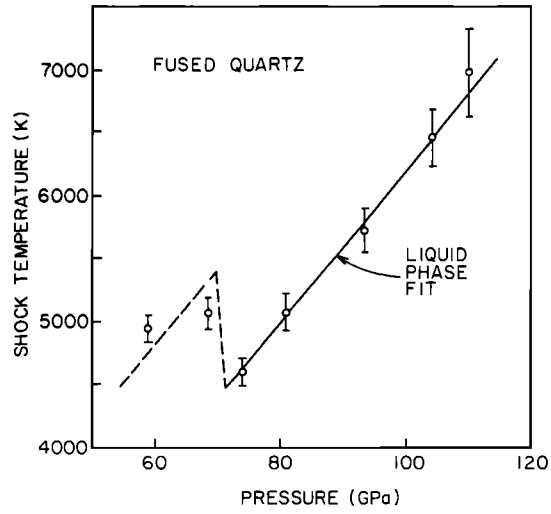

Fig. 3. Measured shock temperatures versus pressure in fused quartz experiments. As in Figure 2, the heavy line represents a calculated liquid phase fit to the experimental temperatures. The data are insufficient to constrain a similar fit for the solid phase, but a representative solid stishovite curve is indicated schematically by a dashed line.

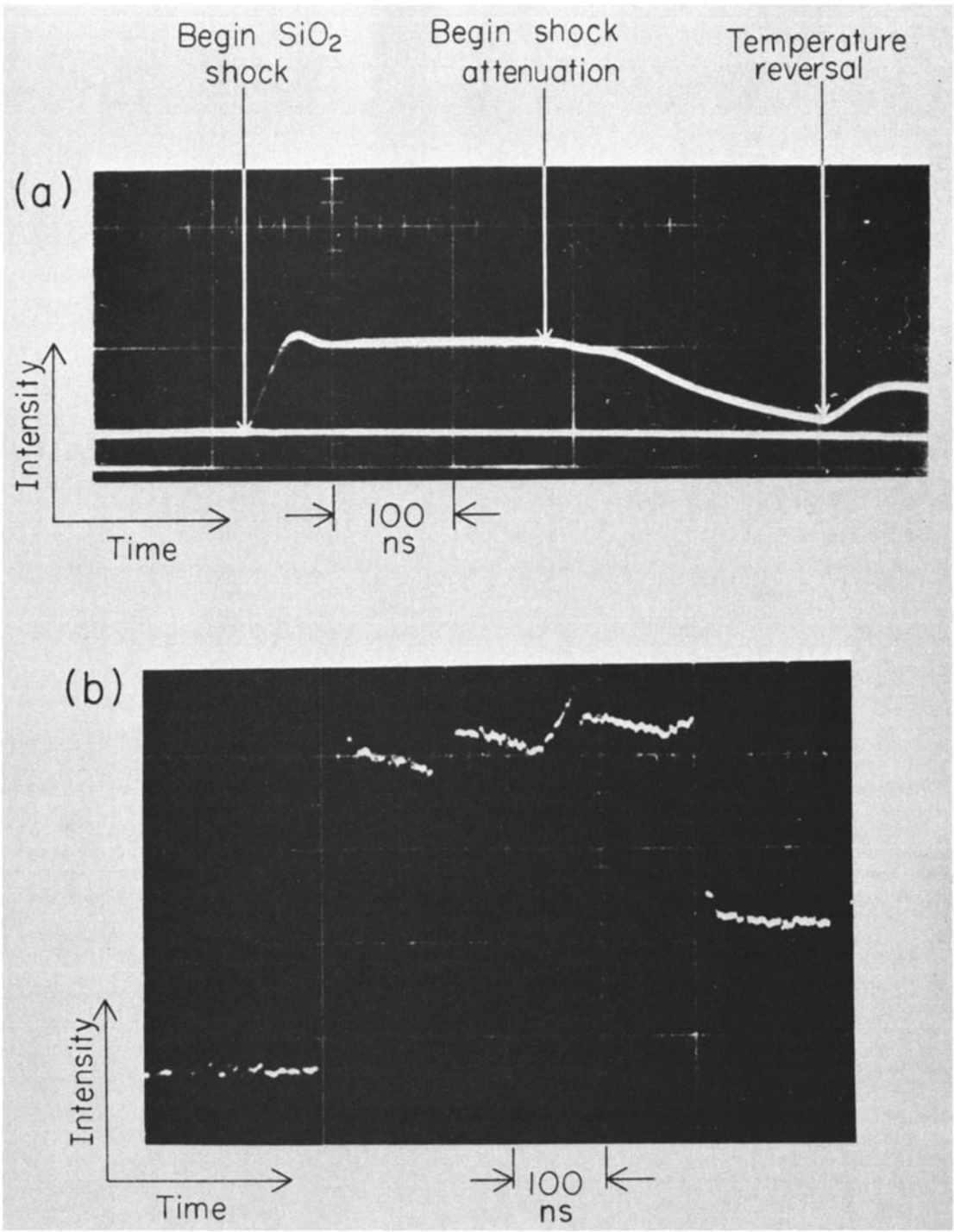

Fig. 4. (a) Light intensity versus time record for fused quartz experiment with decaying shock amplitude. Peak shock pressure is 97.5 GPa. Temperature increase is observed as shock pressure decreases. Wavelength is 500 nm. (b) Intensity record for fused quartz shot at 73.3 GPa pressure. Light intensity fluctuations are observed at this pressure near the shock temperature minimum. Calibration for this 650-nm wavelength record is ~2.2 x 10^3 W m^{-2} sr^{-1} nm^{-1} per division.

Interpretations

The present set of experiments suggest that the high-pressure phase of SiO_2, presumably stishovite, undergoes a shock-induced phase transition which is apparent in shock temperature data for both α-quartz and fused quartz Hugoniot states. Both sets of data display steep temperature declines with increasing pressure. Since the two negative sloping segments do not form a continuous curve, they probably do not represent an equilibrium phase boundary with a negative Clapeyron slope. We prefer the interpretation that the abrupt temperature drop is

TABLE 3. Supplemental SiO_2 Hugoniot Data

Studied Sample	Tantalum Impactor Velocity W, km/s	Sample Shock Velocity (Measured) u_s, km/s	Sample Particle Velocity (Calculated) u_p, km/s	Pressure (Calculated) P, GPa
α-quartz	5.172 ± 0.007	8.64 ± 0.06	4.02 ± 0.01	92.0 ± 0.7
α-quartz	5.62 ± 0.01	9.27 ± 0.16	4.34 ± 0.02	106.5 ± 1.9
α-quartz[a]	5.871 ± 0.010	9.73 ± 0.06	4.51 ± 0.01	116.0 ± 1.4
α-quartz	5.926 ± 0.011	9.70 ± 0.12	4.55 ± 0.01	116.9 ± 1.4
α-quartz	6.297 ± 0.012	9.82 ± 0.10	4.84 ± 0.01	126.0 ± 1.5
α-quartz	6.600 ± 0.012	10.30 ± 0.10	5.05 ± 0.01	137.7 ± 1.5
Fused quartz	5.134 ± 0.007	7.98 ± 0.14	4.17 ± 0.01	73.3 ± 1.3
Fused quartz	5.445 ± 0.009	8.42 ± 0.11	4.397±0.012	81.6 ± 1.1
Fused quartz	5.888 ± 0.011	9.08 ± 0.10	4.716±0.013	94.4 ± 1.0
Fused quartz	6.285 ± 0.007	9.40 ± 0.10	5.023±0.008	104.1 ± 1.1
Fused quartz	6.499 ± 0.010	9.73 ± 0.09	5.175±0.011	111.0 ± 1.0

[a]Data obtained from streak camera records. All others obtained from duration of shock-induced luminescence in temperature shots.

observed because the stishovite phase is metastable, at least on the time scale of the shock rise time, throughout what would otherwise be the mixed phase region of the Hugoniot curve. Finally, at or near the pressure of 100% completion of the phase change, the transition is finally manifested in the state observed by the pyrometer, with the equilibrium temperature reflecting the latent heat of transition. This interpretation allows us to draw the phase line by connecting the temperature minima in the two data sets, as has been shown in Figure 6b. This phase boundary appears to have a small but positive slope, and this, taken with an assumed positive entropy change (estimated from the temperature drops to be of order R per mole of atoms), implies that the transition is accompanied by a modest volume increase.

This observation is not inconsistent with the apparent volume decrease seen in the Hugoniot pressure-volume data above 117 GPa. This is because the volume decrease reflects the adiabatic shift to the equilibrium Hugoniot state of the liquid from that of the relatively less compressible metastable solid. In contrast, the conventional volume increase with melting is a manifestation of the equilibrium between phases at constant pressure and temperature. As pointed out earlier, if the transition were not overdriven but occurred in equilibrium at all pressures, the extrapolated upper branch of the u_s-u_p Hugoniot in Figure 5 would join the stishovite branch continuously at about 70 GPa pressure, which is approximately the pressure at which the observed Hugoniot temperatures first cross the proposed phase boundary.

To summarize the characteristics of the transition seen here, it is apparently accompanied by a small decrease in density, a fairly large positive latent heat, and a 'softening' of the Hugoniot adiabat above the transition pressure. These results are all consistent with the identification of the transition with melting. Stishov [1975] has shown that for simple solids

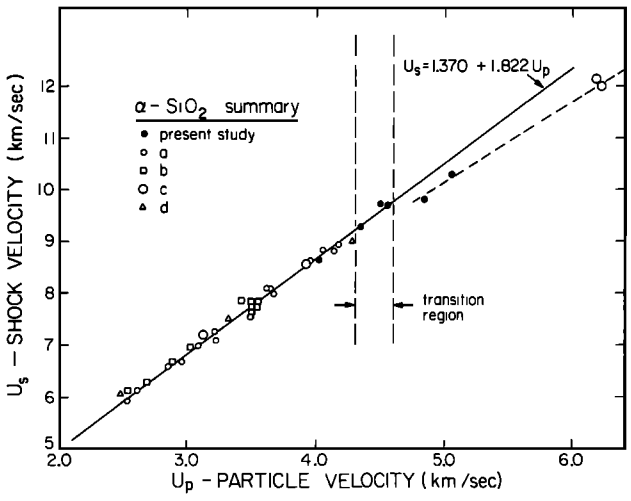

Fig. 5. Summary of α-quartz Hugoniot data plotted in the particle velocity-shock velocity plane. Solid circles are results from the present investigation. Separate linear fits are given for SiO_2 in the stishovite regime and for points above newly observed phase transition. Sources of data are (a) Wackerle [1962], (b) Marsh [1980], (c) Trunin et al. [1971], and (d) Podurets et al. [1976].

TABLE 4. Derived Stishovite Equation of State and Melting Parameters

Parameter	Value
Melting transition (at 70 GPa pressure)	
Melting temperature T_m, K	4500 ± 200
Volume change $\Delta V_m/V$	0.027 ± 0.007
Latent heat of fusion ΔH_m, MJ/kg	2.4 ± 0.6
Melting line slope dT_m/dP, K/GPa	11 ± 5

	Solid	Liquid
Equation of State Parameters		
K_T, GPa	306[a]	242[b]
Grüneisen parameter γ_o	1.38[c]	1.4[b]
exponent n	3.2[b]	0.5[b]
Zero-pressure density ρ_o, g/cm^3	4.2901[a]	4.15[b]
$(dK_o/dP)_s$	5.4[b]	3[b]
E_{tr}, MJ/kg	0.82[d]	2.4[b]
Properties Along Hugoniot		
α-quartz principal Hugoniot S	1.822[b]	1.619[b]
C_o, km/s	1.370[b]	2.049[b]
C_v along α-quartz Hugoniot		
A, kJ kg^{-1} k^{-1}	0.736[e]	0.813[e]
B, kJ kg^{-1} k^{-2}	1.102x10^{-4}[e]	1.418x10^{-4}[e]
C_v along fused quartz Hugoniot		
A, kJ kg^{-1} K^{-1}		1.045[e]
B, kJ kg^{-1} K^{-2}		0.995x10^{-4}

[a]Measured by Weidner et al. [1982].

[b]Fit to shock wave EOS.

[c]Measured by Ito et al. [1974].

[d]Measured by Robie et al. [1978].

[e]Fit to Hugoniot temperatures, this work, compare equation (4).

the entropy of fusion is expected to be of order R per mole of atoms in the limit of high temperature and pressure. Furthermore, it has been well established, for example, by Duvall and Graham [1977], that equilibrium shock-induced melting should appear in the Hugoniot data as a change in slope similar in sign and magnitude to that seen in the SiO_2 results. One approach to quantifying the melting transition is by computing theoretical Hugoniot temperature curves for the liquid phase and comparing them to the experimental results for α-quartz and fused silica.

The calculations of Hugoniot temperatures in this work were performed using the following method. The adiabat of isentropic compression $P_s(V)$ of the phase of interest is obtained through numerical solution of the equation

$$\frac{dP_s}{dV} = \frac{dP'_H}{dV} + \frac{\gamma}{V}\frac{d}{dV}\left(\frac{V}{\gamma}\right)(P'_H - P_s) + \frac{\gamma}{2V}\left[(V_o - V)\frac{dP'_H}{dV} - P'_H - 2P_s\right] \quad (2)$$

Here, P'_H and V_o refer to the 'metastable Hugoniot' of the phase in question (solid or liquid stishovite) centered at STP conditions. This metastable Hugoniot is derivable from the principal Hugoniot as described by McQueen et al. [1967] and depends upon the magnitude of the transition energy E_{tr} at standard conditions.

In the present work, an interpolation formula was fit to the metastable Hugoniot, and (2) was solved for $P_s(v)$, the isentrope. Given $P_s(v)$, the

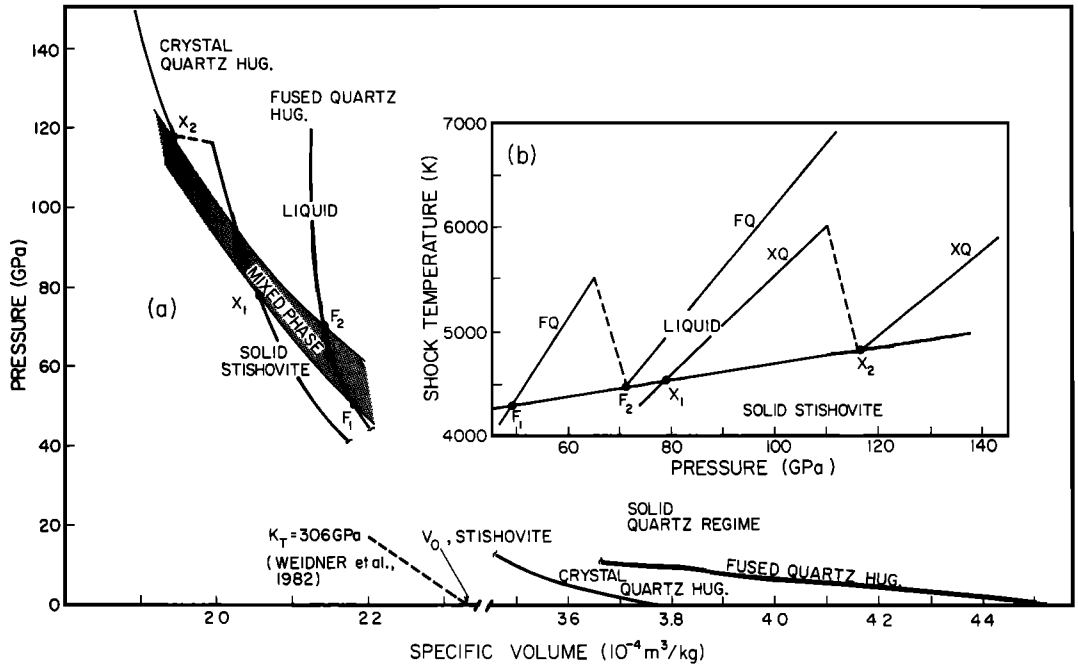

Fig. 6. (a) Pressure-volume Hugoniot curves for SiO_2 starting in α-quartz and fused quartz initial states. X_1 and X_2 denote the onset and completion of the transition from stishovite to liquid along the α-quartz Hugoniot. F_1 and F_2 are the corresponding points along the fused quartz Hugoniot. For orientation, the zero-pressure volume and isothermal bulk modulus of solid stishovite are shown, and the inferred region of mixed solid and liquid phases is shaded. Note that the cusp which occurs in the α-quartz Hugoniot at X_2 may have its fused quartz counterpart at F_2, but the present data are not sufficient to resolve this feature. (b) Correlative temperature-pressure plot, showing temperatures along the fused quartz (FQ) and crystalline quartz (XQ) Hugoniots. In this plane, points F_2 and X_2 define the location of the phase line, and points F_1 and X_1 are derived from it.

shock temperature T_H was found at various values of V through solution of

$$\int_{T_s}^{T_H} C_v dT = \frac{V}{\gamma} (P_H - P_s) \qquad (3)$$

where now P_H is the principal Hugoniot pressure and T_s is the temperature on the isentrope at specific volume V.

The shock temperatures of the liquid (stishovite) computed in this way prove to be insensitive to the assumed value of the Grüneisen parameter $\gamma = V (\partial P/\partial E)_V$ because of the lack of an independent constraint for the reference isentrope. For the liquid state, any a' priori value, of order unity, yields essentially indistinguishable results. For the current calculations, values of $\gamma_0 = 1.4$ and $n = 0.5$ are used and come from consideration of fused quartz and α-quartz shock wave data in the liquid range, which together are used to derive self-consistent equation of state parameters. These parameters are only loosely constrained, but they do provide a useful reference for comparison with experiment. Also derived from this equation of state is a value of $E_{tr} = 2.4$ MJ/kg for the transition energy of a hypothetical metastable liquid. As with the γ values, this provisional value simply provides a guide for calculation, whereas more rigorous determinations of the transition thermodynamics are considered below.

The computed Hugoniot temperature profiles are quite sensitive to the assumed value and variation of the specific heat C_v. A feature of the experimental results reported here is that in each of the phase regions the temperature-pressure points are well fit by a linear relation. This experimental fact cannot be reconciled with a constant or simple Debye form of the specific heat. We therefore report here the empirical C_v value which fits the data along the Hugoniot, assuming that $E_{tr} \approx 2.4$ MJ/kg for the α-SiO_2 to hpp (liquid) transition. The form of C_v used is that suggested by Wallace [1972].

Along the fused quartz Hugoniot, in the inferred liquid range, the data fit

$$C_v = A + BT \qquad (4)$$

with $A = 1.045$ kJ kg^{-1} K^{-1} and $B = 9.95 \times 10^{-5}$ kJ kg^{-1} K^{-2}. Similarly, the liquid data along the α-quartz Hugoniot yield a specific heat of the form of (4) with $A = 0.813$ and $B = 1.418 \times 10^{-4}$ (same SI units). In addition, there are enough data on the α-quartz Hugoniot which give the temperature of solid stishovite, in order to derive an empirical specific heat for that phase. Along the α-quartz Hugoniot, we obtain, for stishovite, $A = 0.736$ and $B = 1.102 \times 10^{-4}$.

When evaluated near the inferred melting

temperature of ~4500K, the stishovite fit yields a specific heat very close to the classical value of 3R (= 1.245 kJ kg^{-1} K^{-1} in this case). Both of the liquid fits yield higher than classical values of $C_v \approx 3.5R$ near the melting point. Also noteworthy is a marked increase in C_v with increasing temperature. In the case of liquid along the fused quartz Hugoniot, at 7000 K, C_v reaches ~4.4R in this model.

If the Hugoniot curves of fused and α-quartz each pass through phase regions corresponding to solid stishovite, liquid, and mixed phases, intercomparison of the Hugoniot curves for these different initial states should provide important corroborative information on the occurrence and energetics of the inferred melting transition. More specifically, the available Hugoniot data, plotted in the P-V plane taking into account the 'delayed' transition onset inferred from the temperature data, can provide a picture of the solid-liquid-mixed phase boundaries. Figure 6 is a plot of these data for SiO_2 above 40 GPa pressure.

Plotted in Figure 6a are the pressure-volume Hugoniot curves for α-quartz and fused silica. These smoothed Hugoniots have been obtained by transformation of the u_s-u_p fits to the shock wave data as given above. The α-quartz Hugoniot is shown here as discontinuous around 117 GPa pressure, this reflecting the discontinuity between the two linear fits as shown in Figure 5.

In the case of fused quartz, either the existing shock wave data are of too low resolution, or the effects of shock heating and thermal pressure are too great to allow detection of similar discontinuities due to overdriving. In this case, it is expedient to plot a single curve which best represents the somewhat scattered Hugoniot data. Drawing from the compilation of fused quartz shock wave data by Marsh [1980] and those tabulated here (Table 3), the Hugoniot is assumed described by

$$u_s = 0.0592\ u_p^2 + 1.279\ u_p + 1.528 \text{ km/s} \quad (5)$$

for pressures above 40 GPa. The transformation of this fit is plotted in Figure 6a.

Along the α-quartz Hugoniot in Figure 6a, points X_1 and X_2 are labeled as the points of onset and completion of melting of stishovite. The corresponding points in the temperature-pressure plane are labeled in the inset, Figure 6b. As is suggested by plots, the Hugoniot crosses into the field of temperatures and pressures where, under equilibrium conditions, the material would be liquid. The metastability of solid under shock conditions is such that not until ~117 GPa pressure does the equilibrium liquid state appear at point X_2.

Similarly for fused quartz, points F_1 and F_2 in Figures 6a and 6b show the onset and completion of melting along the Hugoniot. In the P-T plot of Figure 6b, the phase boundary is simply the line constructed by joining points X_2 and F_2, while points X_1 and F_1 are defined by the intersection of this line with the 'lower branches' of the temperature Hugoniots.

Now in the pressure-volume plane (Figure 6a), the boundary between phases is a 'band' within which a mixed phase assemblage is the equilibrium state. The mixed phase region is therefore the band of P-V states between the curves connecting points X_1 and F_1 and points X_2 and F_2 as shown.

This construction yields valuable information concerning the phase transition. Within the region of mixed phases, the Gibbs phase rule dictates that at a fixed pressure the temperature must remain fixed. Thus at any pressure the horizontal width of the mixed phase band is the volume change of transition (in this case, fusion) at constant T and P.

The width of the mixed phase band is best constrained by observations near a pressure of ~70 GPa, since points X_1 and F_2 both fall near this pressure. At 70 GPa pressure, we obtain a volume change of $\Delta V = (0.057 \pm 0.015) \times 10^{-4}$ m^3/kg, or a relative volume increase of 2.7%.

In addition, further consideration of Figure 6 yields an estimate for the latent heat of fusion. The internal energies of states on the solid and liquid extremes of the mixed phase band can be obtained from the Hugoniot energies, corrected to the appropriate P-V states. The latent heat ΔH_m is simply the difference between these internal energies plus an amount of energy $P\Delta V$ equal to the work done in melting at constant pressure.

Once again, evaluating the appropriate quantities at 70 GPa pressure, the liquid internal energy is given by the fused quartz Hugoniot energy at that pressure, $E_H = E_o + 1/2\ P_H\ (V_o - V)$. Using α-quartz at STP as the reference state of energy, this value is 8.47 MJ/kg. The solid internal energy is given by the α-quartz Hugoniot energy at 65 GPa plus the Mie-Grüneisen correction for the 5-GPa offset between the Hugoniot and the melting state at the same volume. This amounts to 6.47 MJ/kg. Thus the difference of 2.0 MJ/kg plus the work term $P\Delta V$ = 0.4 MJ/kg yields a latent heat of fusion of 2.4 MJ/kg. Considering the uncertainties in the Hugoniot densities and energies from which this value is derived, the uncertainty in ΔH_m is approximately ±25%.

This result is of the expected size, corresponding to an entropy change $\Delta S \approx 1.3R$ in fair agreement with the predictions of the melting systematics of Stishov. Furthermore, the values of ΔH_m and ΔV derived here combined to yield a Clapeyron melting slope of $(dT/dP)_m \approx 11$ K/GPa, which makes the melting line interpretation of Figure 6 self-consistent. While the calculated melting line slope has been shown to be consistent with the slope seen in the Hugoniot temperature data, this self-consistency may not be compelling evidence for the correctness of this interpretation. In order to independently calculate one or more of the above properties of the proposed melting transition we employ the Lindemann melting law to derive the melting line slope.

The Lindemann melting law, a semiempirical theory of melting, predicts the volume dependence of the melting temperature on the basis of the amplitudes of atomic lattice vibrations. It can be used to estimate the trajectory of the melting line of a solid if the volume dependence of its vibrational spectrum is known. Grover [1971] has shown that for metals the Grüneisen parameter γ for the solid phase adequately describes this dependence, and the Lindemann law in this formulation becomes

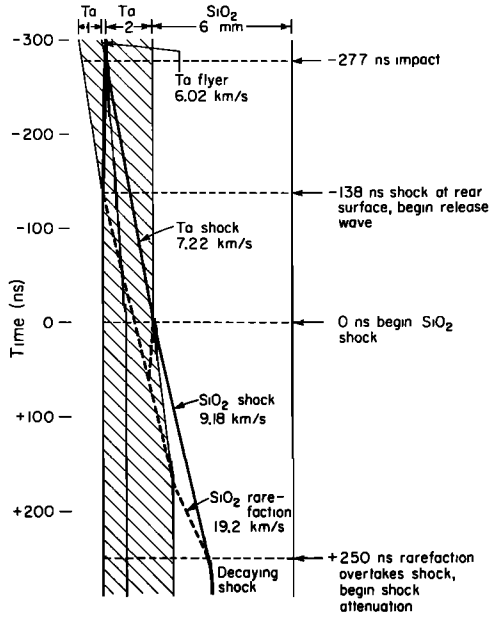

Fig. 7. Graphical position-time representation of the decaying shock experiment shown in Figure 4a. Determination of rarefaction wave velocity allows calculation of the Grüneisen parameter γ. Heavy lines are trajectories of shock waves in the tantalum driver and fused quartz sample. Dashed lines are release waves propagating at longitudinal sound speed.

$$- d(\ln T_m)/d(\ln V) = 2\gamma - 2/3 \qquad (6)$$

If we assume that this holds for SiO_2, taking the value for stishovite $\gamma = 0.97$, the right-hand side of the above equation is ~1.27. Now it may be shown that the pressure derivative of the melting temperature becomes

$$\frac{dT_m}{dP} = \left(\frac{\partial T}{\partial P}\right)_V \left\{1 - \left[\frac{T}{V}\left(\frac{\partial V}{\partial T}\right)_P (2\gamma - 2/3) + 1\right]^{-1}\right\} \qquad (7)$$

Evaluating this expression at $V = 2.075 \times 10^{-4}$ m^3/kg, using a coefficient of thermal expansion $\alpha = 1 \times 10^{-5}$ K^{-1}, $T = 4500$ K, and $P = 70$ GPa, we obtain $dT_m/dP \approx 9.0$ K/GPa. If $\alpha = 1.5 \times 10^{-5}$ K^{-1}, as determined at low pressure by Ito et al. [1974], then ~14 K/GPa is obtained. This agreement with the above determined Clapeyron slope gives weight to the stishovite melting hypothesis.

The Grüneisen parameter γ is another parameter of the thermal equation of state whose value may be refined from a consideration of the present data. The high-pressure value of γ for the liquid phase may be estimated from an analysis of the decaying shock, fused quartz experiment illustrated in Figure 4a. The sound speed for states along the Hugoniot is given as [McQueen et al., 1967]

$$C_H = V\left\{\left.\frac{dP}{dV}\right|_H \left[(V_o - V)\frac{\gamma}{2V} - 1\right] + P_H \frac{\gamma}{2V}\right\}^{1/2} \qquad (8)$$

The subscript H denotes quantities evaluated on the Hugoniot at volume V. Since C_H is the velocity with which a rarefaction wave propagates with respect to the shocked material, knowledge of the time required for an overtaking rarefaction to reach the shock front allows a calculation of C_H and γ for the shocked state.

Figure 7 is an X-t diagram in which time increases vertically downward and the horizontal direction represents the positions of target and impactor during the collision process. The trajectories of the shock waves and overtaking release waves may be seen schematically, and for the present case, the shock attenuation in the SiO_2 layer begins at a time dependent upon the SiO_2 rarefaction speed. The experimentally observed time of this event is approximately 250 ns after the shock enters the SiO_2, which requires the rarefaction to propagate at 19.2 km/s in the laboratory reference frame, or 14.4 km/s with respect to the material which is moving with particle velocity 4.8 km/s. Applying equation (8) to this result, $\gamma \approx 1.6 \pm 0.2$ for liquid SiO_2 at 97.5 GPa on the fused quartz Hugoniot. This agrees reasonably well with the liquid γ value used above in the theoretical calculations.

The above calculations depend upon knowledge of the equation of state parameters of the tantalum flyer plate and base plate. Tantalum (density 16.66 g/cm^3) shock and sound velocities used here were calculated from the fit to the Hugoniot data

$$u_s = (1.298 \pm 0.012)u_p + (3.13 \pm 0.025) \text{ km/s} \qquad (9)$$

of Mitchell et al. [1979] (see also, Mitchell and Nellis, 1981), and by assuming that the Grüneisen γ varies in direct proportion to V/V_o, with a zero-pressure value of 1.69 [Walsh et al., 1957]. Uncertainties in these quantities affect the calculated value of γ for SiO_2.

Table 4 summarizes the properties of the newly inferred melting transition and of what is known of the high-pressure liquid phase. The following is a brief summary of the sources or inferences from which these conclusions are derived. The melting transition and its temperature are identified directly by the shock temperature observations. Crucial to this interpretation is the assumption that the minima of the temperature drops seen in both data sets directly measure the equilibrium melting temperature, whereas the 'peak' values, which are ~1000 K higher, reflect a metastable untransformed state. Supportive of this interpretation is the fact that theoretical Hugoniot temperatures assuming a plausible liquid transition energy and equation of state fit the data adequately.

Volume change and latent heat of fusion are derived by transforming the melting states identified in the P-T plane into the P-V plane with the aid of existing shock wave data. From this follows the dual constraint of the melting line slope, both directly from P-T observations and from the Clausius-Clapeyron relation. Lindemann law predictions further agree with this result.

Specific heat of the high-pressure SiO_2 liquid is not rigorously constrained, but all reasonable interpretations of the temperatures observed require large values (compared with the Dulong-Petit value) which increase with increasing shock temperature. While data constraining the Grüneisen parameter of the liquid are also sparse

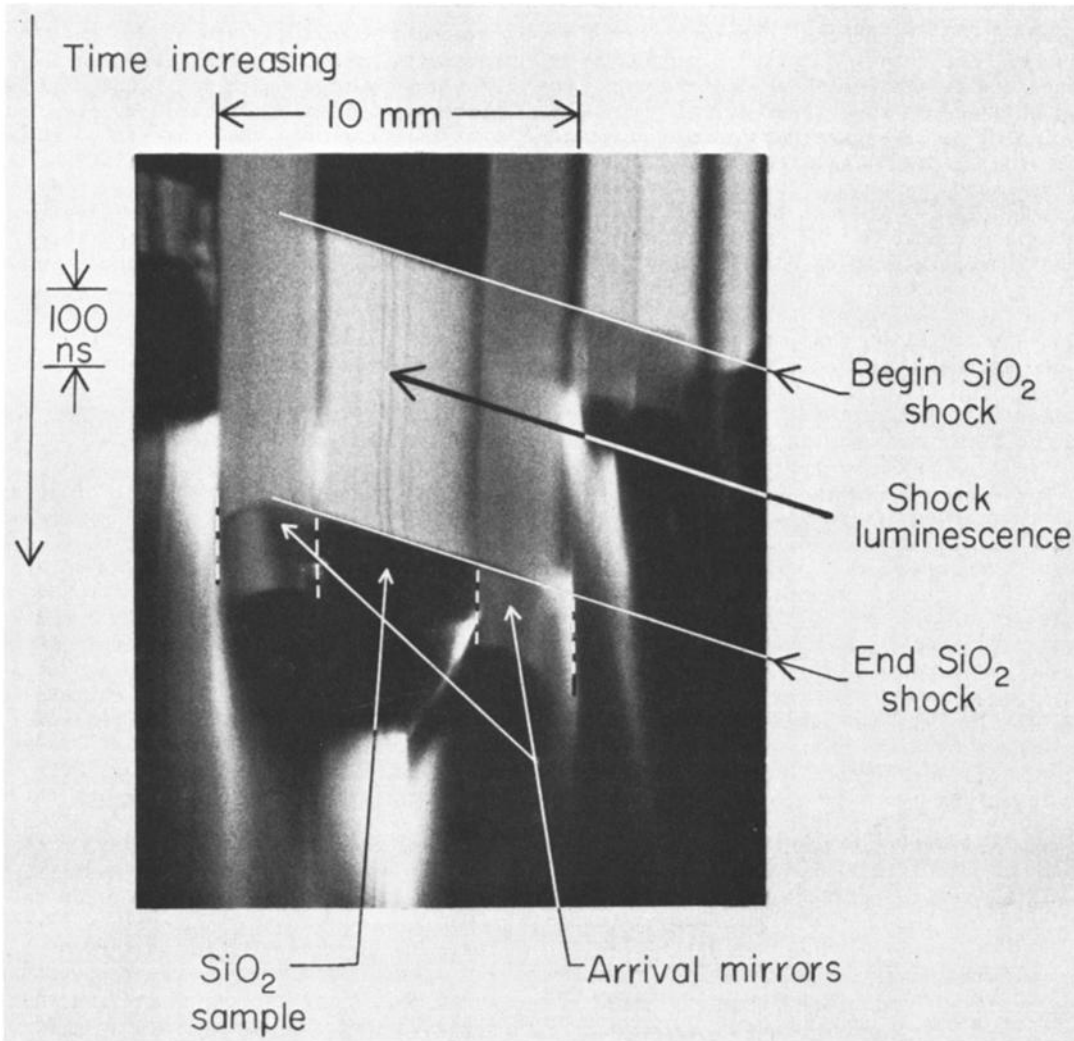

Fig. 8. Image converter streak camera record of shock luminescence in α-quartz shocked to 106.5 GPa pressure. Horizontal dimension is lateral distance across the sample face. In addition to determining shock velocity in sample, this photograph was intended to record any spatial or time variation in light intensity arising from local temperature inhomogeneities. No evidence of heterogeneous thermal distribution is detected.

compared with those available for solid stishovite, the quoted value derived from the sound speed is consistent with reasonable equations of state.

It is appropriate at this point to discuss some of the limitations of the current experimental technique and the assumptions which are implicit in the interpretations discussed here. Perhaps the most crucial issue in this regard is the question of the source of the observed blackbody radiation and whether that source is truly representative of the Hugoniot state as claimed. Experimental evidence suggests that the light observed in these experiments originates in a thin layer near or coincident with the shock front. The chief evidence for this is the extremely rapid (<5 ns) rise and fall times observed for the radiation, which would not be observed if the light source were distributed throughout a larger volume of the sample. These observations are in apparent conflict with those of Kormer [1968] in which substantially longer rise times were seen in shocked alkali halides. Those earlier observations were made, however, at lower pressures and with less time resolution than the current studies, so that the disagreement may not be significant. Subsequent experiments using the present apparatus with NaCl samples have produced signals qualitatively identical with the SiO_2 results [Lyzenga, 1982].

As discussed in that paper, the microscopic mechanism of thermal radiation in these experiments is likely to be related to shock-generated electronic defects and the promotion of electrons to conduction states. The strength of the shock wave has a profound effect upon the equilibrium population and temperature of these radiating electrons. As Kormer showed, for a sufficiently strong shock, an effectively opaque electronic layer may be achieved on a time scale short compared with the time required for temperature equilibration of the electrons with the atomic lattice. In such extreme cases, the observed temperature is lower than that of the actual Hugoniot state.

This discussion has significance for the

present case of SiO_2 shock temperatures. The observation of superheated solid temperatures above the equilibrium melting point can be understood if a longer time is required for the equilibration of a segregated assemblage of mixed phases than the electron temperature equilibration time. As stated by Lyzenga [1982], this latter time is estimated to be of the order of 10^{-9}s. Above the pressure of complete shock melting, the single phase temperature is once again reflected in the radiated spectrum, in this model.

One final issue regarding the source of the shock-induced radiation has to do with the question of heterogeneous yielding and temperature deposition in quartz. Several investigators [e.g., Neilson et al., 1962; Grady, 1977] have discussed the localized heating and luminescence which occurs in narrow `shear bands' when α-quartz is shock loaded at relatively low pressures. This behavior is observed at pressures well below the stishovite pressure regime. If heterogeneous heating occurs in a sample, optical pyrometry will generally yield an apparent temperature, characteristic only of the localized `hot spots' with a correspondingly lower emissivity. In such a case, the apparent temperature would be significantly higher than that actually characteristic of the bulk sample.

While this behavior is not expected to persist through the extremely high pressures and phase transitions of these experiments, an effort has been made to search for this effect. Figure 8 is a reproduction of a streak camera record from an α-quartz equation of state experiment at 106.5 GPa pressure. The record presents a time history of the light emerging (or reflected) from a strip across the back surface of the target. As the image of this slit is swept down across the cathode ray tube recording screen, the onset and termination of shock luminescence is clearly seen during shock wave transit through the SiO_2 sample. The inclination of the observed shock arrivals is due to tilt of the impacting flyer plate with respect to the target. Within the resolution of the photographic record, the light intensity is spatially uniform and constant throughout the record. The faint dark vertical lines are scan line artifacts from the image converter tube face. If temperature inhomogeneities exist at all, they must be on a scale of microns or smaller.

Conclusions and Implications

The observation of melting in stishovite at pressures near 1 Mbar (100 GPa) and the estimation of the latent heat of fusion have significant implications for the conditions existing in the earth's lower mantle, although, as an end-member in the MgO-FeO-SiO_2 system, it is unlikely that stishovite is present as a pure phase. Knowledge of the melting temperatures of candidate constituents of the mantle allows constraints to be placed on the geotherm in the solid mantle and further allows the estimation of such quantities as creep viscosity which may have a temperature dependence which scales with the melting point.

Kennedy and Higgins [1972] have made arguments concerning the melting temperature of mantle material using a simplified model of this material as a binary eutectic system with MgO and SiO_2 as end-members. If the melting temperature of the pure substances is known at the pressure of interest, the liquidus temperature of the idealized mantle material should lie at lower temperatures. Kennedy and Higgins further argue that the depth of the eutectic minimum at low pressures should be a lower limit to the depth of the trough at high pressures. Applying this reasoning to SiO_2, with a melting temperature of 4800 K, the solidus temperature of the hypothetical binary system might be no higher than about 3500 K. This estimate is based upon the 1305 K difference between the lowest observed melting temperature in the SiO_2 (quartz)-MgO(periclase) system (1820 K) and that of periclase (3125 K), following the reasoning of Weertman [1970]. This neglects the possibility of more complex configurations than a simple single eutectic trough.

These results indicate that in order for a silica-bearing mantle to be solid at pressures near the core-mantle boundary, the temperature may be required to be at or below ~3500 K.

The melting temperature of stishovite at mantle pressures also provides a basis for discussing the rheology and creep of silicate mantle mineral assemblages. Again, although stishovite is unlikely to be present in the earth's lower mantle as a discrete phase, since it has the octahedral coordination of Si^{4+} with O^{2-} common to all proposed lower mantle silicates, its rheological properties may provide analogs of the minerals of the lower mantle. If the temperature of the geotherm and its relation to the melting temperature of the mantle are known, estimates of effective viscosity in creep due to deep mantle convection may be derived. Since present data are for only one component of what might be considered a simplified SiO_2-MgO system representation of the lower mantle, inferences regarding the effect of pressure on viscosity should be considered indicative rather than determinative.

For the purpose of estimating the effect of compression on lower mantle viscosity, we employ the semiempirical relation given by Weertman [1970], relating the rate of diffusion-controlled creep to the temperature and melting point. For a given stress level and strain rate, this relation may be expressed in terms of effective viscosity η:

$$\eta = C \exp (gT_m/T) \qquad (10)$$

Here, g is a constant taken by Weertman to be ~18 for most metals. Sammis et al. [1981] show that for both metals and olivine this empirical correlation adequately describes experimental results for diffusion activation parameters. C is a constant, while T and the melting point T_m vary with depth in the mantle, according to the assumed geotherm and melting point gradient.

Evaluating the appropriate gradients at a depth in the lower mantle corresponding to 70 GPa pressure (~1600 km), we can obtain values of $d\ell n\eta/dz$, the rate of viscosity variation with depth, z. Using reasonable adiabatic temperature profiles (with $T \approx 3000$ at 70 GPa) and $dT_m/dP = 10$ K/GPa, we obtain $d\ell n\eta/dz \approx 7 \times 10^{-4}$ km^{-1}. If we allow the rather larger than observed melting point gradient of $dT_m/dP = 20$ K/GPa, this increases to 3.8×10^{-3} km^{-1}.

Taking these gradients as limits throughout the

depth of the lower mantle, the expected total variation in η is by a factor of between 4 and 2000. This result applies to pure stishovite, strictly speaking, but serves to illustrate the dramatic effect on viscosity gradients which may be expected as a result of a low value of dT_m/dP in the actual mantle. Thus, if the observed melting point gradient in stishovite may be applied to the earth's mantle, it would seem unlikely that the effective viscosity could increase by more than a factor of $\sim 10^3$ between the top and bottom of the lower mantle.

Acknowledgments. We appreciate the cooperation and collaboration of personnel at Lawrence Livermore Laboratory (LLL) in use of the light gas gun and related facilities, especially that of W. J. Nellis. J. Trainor and M. B. Boslough provided valuable assistance in obtaining pyrometer calibrations. We also appreciate the helpful discussions and suggestions of J. Shaner, R. G. McQueen, J. N. Fritz, and J. W. Hopson of Los Alamos Scientific Laboratory in providing their data in preprint form. We also thank R. Jeanloz, E. Stolper, D. L. Anderson, and C. G. Sammis for helpful discussions and suggestions. The technical assistance of J. R. Long, E. Gelle, and M. Long of Caltech and that of D. Bakker, J. Samuels, and W. C. Wallace of LLL is gratefully acknowledged. Support was provided through NSF grant EAR78-12942. Contribution 3433, Division of Geological and Planetary Sciences, California Institute of Technology.

References

Ahrens, T. J., Dynamic compression of earth materials, Science, 207, 1035-1041, 1980.

Davison, L., and R. A. Graham, Shock compression of solids, Phys. Rep., 55, 255-379, 1979.

Duvall, G. E., and R. A. Graham, Phase transitions under shock-wave loading, Rev. Mod. Phys., 49, 523-579, 1977.

Fowles, G. R., Attenuation of the shock wave produced in a solid by a flying plate, J. Appl. Phys., 31, 655-661, 1960.

Grady, D. E., High Pressure Research: Applications to Geophysics, edited by M. Manghnani and S. Akimoto, pp. 389-438, Academic, New York, 1977.

Grover, R., Liquid metal equation of state based on scaling, J. Chem. Phys., 55, 3435-3441, 1971.

Ito, H., K. Kawada, and S. I. Akimoto, Thermal expansion of stishovite, Phys. Earth Planet. Inter., 8, 277-281, 1974 (Erratum, Phys. Earth Planet. Inter., 8, 277-281, 1975.)

Jones, A. H., W. M. Isbell, and C. J. Maiden, Measurement of the very high pressure properties of materials using a light-gas gun, J. Appl. Phys., 37, 3493-3499, 1966.

Kennedy, G. C., and G. H. Higgins, Melting temperatures in the earth's mantle, Tectonophysics, 13, 221-232, 1972.

Kormer, S. B., Optical study of the characteristics of shock-compressed condensed dielectrics, Sov. Phys. Usp., Engl. Transl., 11, 229-254, 1968.

Lyzenga, G. A., Optical pyrometry at high shock pressures and its interpretation, in Shock Waves in Condensed Matter-1981, edited by W. J. Nellis, L. Seaman, and R. A. Graham, pp. 268-276, American Institute of Physics, New York, 1982.

Lyzenga, G. A., and T. J. Ahrens, A multi-wavelength optical pyrometer for shock compression experiments, Rev. Sci. Instrum., 50, 1421-1424, 1979.

Lyzenga, G. A., and T. J. Ahrens, Shock temperature measurements in $Mg SiO_4$ and SiO_2 at high pressures, Geophys. Res. Lett., 7, 141, 1980.

Marsh, S. P., LASL Shock Hugoniot Data, 680 pp., University of California Press, Berkeley, 1980.

McQueen, R. G., J. N. Fritz, and S. P. Marsh, On the equation of state of stishovite, J. Geophys. Res., 68, 2319-2322, 1963.

McQueen, R. G., S. P. Marsh, and J. N. Fritz, Hugoniot equation of state of twelve rocks, J. Geophys. Res., 72, 4999-5036, 1967.

Mitchell, A. C. and W. J. Nellis, Shock compression of aluminum, copper, and tantalum, J. Appl. Phys. 52, 3363-3374.

Mitchell, A. C., W. J. Nellis, and B. L. Hord, Tantalum Hugoniot measurements to 430 GPa (4.3 Mbar) (abstract), Bull. Am. Phys. Soc., 24, 719, 1979.

Neilson, F. W., W. B. Benedick, W. P. Brooks, R. A. Graham, and G. W. Anderson, Les Ondes de Detonation, edited by G. Ribaud, Editions du Centre National de la Recherche Scientifique, Paris, 1962.

Podurets, M. A., L. V. Popov, A. G. Sevast'yanova, G. V. Simakov, and R. F. Trunin, On the relation between the size of studied specimens and the position of the silica shock adiabat, Izv. Acad. Sci. USSR Phys. Solid Earth, Engl. Transl., no. 11, 59-60, 1976.

Robie, R. A., B. S. Hemingway, and J. R. Fisher, Thermodynamic Properties of Minerals and Related Substances at 298.15 K and 1 Bar (10^5 Pascals) Pressure and at Higher Temperatures, pp. 216-221, Government Printing Office, Washington, D. C., 1978.

Sammis, C. G., J. C. Smith, and G. Schubert, A critial assessment of estimation methods or activation volume, J. Geophys. Res., 86, 10707-10718, 1981.

Stishov, S. M., The thermodynamics of melting of simple substances, Sov. Phys. Usp., Engl. Transl., 17, 625-643, 1975.

Trunin, R. F., G. V. Simakov, M. A. Podurets, B. N. Moiseyev, and L. V. Popov, Dynamic compressibility of quartz and quartzite at high pressure, Izv. Acad. Sci. USSR Phys. Solid Earth, Engl. Transl., no. 1, 13-20, 1971.

Wackerle, J., Shock-wave compression of quartz, J. Appl. Phys., 33, 922-937, 1962.

Wallace, D. C, Thermodynamics of Crystals, 484 pp, John Wiley, New York, 1972.

Walsh, J. M., M. H. Rice, R. G. McQueen, and F. L. Yarger, Shock-wave compression of twenty-seven metals: Equations of state of

metals, Phys. Rev., 108, 196-216, 1957.
Weertman, J., The creep strength of the earth's mantle, Rev. Geophys. Space Phys., 8, 145-168, 1970.
Weidner, D. J., J. D. Bass, A. E. Ringwood, W. Sinclair, The single-crystal elastic moduli of stishovite, J. Geophys. Res., 87, 4740-4746, 1982.

(Received May 5, 1981 ;
revised October 1, 1982 ;
accepted December 3, 1982.)